



Contents lists available at ScienceDirect

## Sensors and Actuators B: Chemical

journal homepage: [www.elsevier.com/locate/snb](http://www.elsevier.com/locate/snb)



# DNA-based fiber optic sensor for direct *in-vivo* measurement of oxidative stress

Probir Kumar Sarkar<sup>a</sup>, Animesh Halder<sup>a</sup>, Aniruddha Adhikari<sup>a</sup>, Nabarun Polley<sup>a</sup>,  
Soumendra Darbar<sup>c</sup>, Peter Lemmens<sup>b</sup>, Samir Kumar Pal<sup>a,\*</sup>

<sup>a</sup> Department of Chemical, Biological and Macromolecular Sciences, S. N. Bose National Centre for Basic Sciences, Block JD, Sector III, Salt Lake, Kolkata, 700106, India

<sup>b</sup> Institute for Condensed Matter Physics, and Laboratory for Emerging Nanometrology, TU Braunschweig, Mendelssohnstrasse 3, 38106 Braunschweig, Germany

<sup>c</sup> Research & Development Division, Dey's Medical Stores (Mfg.) Ltd., 62, Bondel Road, Ballygunge, Kolkata, 700019, India

### ARTICLE INFO

#### Article history:

Received 5 June 2017

Received in revised form 27 August 2017

Accepted 4 September 2017

Available online xxx

#### Keywords:

DNA-based biomaterial

Fiber optic sensor

Reactive oxygen species

In-vivo oxidative stress measurement

Oxidative stress

### ABSTRACT

Oxygen is one of the most significant elements for life because almost all living organisms utilize oxygen for respiration and energy generation. However, some derivatives of oxygen including free radicals called reactive oxygen species (ROS) are detrimental and cause several diseases such as neurodegeneration, diabetes, cancer and atherosclerosis. Oxidative stress is essentially an inability of our body to counteract or detoxify the harmful effects of ROS through neutralization by antioxidants. Till date direct *in-vivo* measurements of oxidative stress are challenging. In this work, we have developed a novel 2,7-dichlorodihydrofluorescein (DCFH) impregnated genomic DNA-based biomaterial, which is completely insoluble in water and forms excellent thin film layers on optical fiber tips. The biomaterial-sensitized fiber tip fluoresces brightly in the proximity of ROS as the entrapped DCFH is oxidized to highly fluorescent DCF. We have demonstrated that an indigenously developed biomaterial-sensitized optical fiber tip can work as an efficient ROS/oxidative stress sensor in an aqueous medium as well as in the blood phantom (hemoglobin solution). A preclinical study on the minimally invasive direct *in-vivo* oxidative stress detection in mice model has also been successfully demonstrated.

© 2017 Elsevier B.V. All rights reserved.

## 1. Introduction

Molecular oxygen is one of the most important elements for living beings on the earth because almost all living organisms utilize oxygen for respiration and energy generation. But oxygen's derivatives, reactive oxygen species (ROS), can be very detrimental. The generation of ROS has been implicated in the onset and progression of several diseases (e.g., neurodegeneration, diabetes, cancer, and atherosclerosis) [1]. These species were thought only to be released in host defence roles by phagocytic cells; however, it is now clear that at molecular level, ROS exhibit signaling and cell-function-modifying roles for many biological systems [2,3]. They are easily inter-converted and can subsequently react with larger biological molecules, causing chain reactions to occur, which can lead to changes in both the function and structure of cellular components. Oxidative stress is essentially an imbalance

between the production of ROS and the ability of our body to counteract or detoxify the harmful effects through neutralization by antioxidants. Several analytical approaches have been used to detect ROS using nanoparticles, chemiluminescence, various fluorescence probes, mass spectrometry probes etc [4,5]. However, all of the techniques have some relative advantages as well as disadvantages too. Among these fluorescence probes, 2,7-dichlorodihydrofluorescein diacetate (DCFH-DA) is the most widely used one for detection of intracellular oxidative stress. The probe is added to cells in culture and the intracellular oxidation of 2,7-dichlorodihydrofluorescein (DCFH) results in formation of a fluorescent product, 2,7-dichlorofluorescein (DCF), which can be monitored by several fluorescence-based techniques (confocal microscopy, spectroscopic fluorescence detection, flow cytometry etc.) [6,7]. The increased fluorescence intensity usually reflects the presence of ROS in the cells. This type of fluorescence techniques using some specific fluorophores are usually applied for detecting oxidative stress in cellular environment [8,9]. However, use of these fluorescent probes in applications such as *in-vivo* measurement of oxidative stress is sparse in the literature. Direct *in-vivo*

\* Corresponding author.

E-mail address: [skpal@bose.res.in](mailto:skpal@bose.res.in) (S.K. Pal).

measurement of oxidative stress using specific fluorescence probes with negligible additional cytotoxicity remains a great challenge to the researchers. Some other analytical techniques for oxidative stress detection such as nuclear magnetic resonance (NMR), electron paramagnetic (spin) resonance (EPR), derivatization with attendant mass spectrometric (MS) analysis and liquid scintillation counting can also be quite useful but are less portable and often require highly trained technical expertise making the techniques to be highly expensive [7]. The aforementioned factors encourage us to develop a cost effective, simple, efficient and non-invasive or minimally-invasive technique for direct oxidative stress measurement.

The combination of optical fiber-based probes and DNA-based biomaterial offers an attractive non-invasive or minimally-invasive novel approach for various applications in biomedical and environmental sensor design [10,11]. In this study we have attached a fluorescent probe to the fiber tip surface through DNA-based biomaterial matrix assuring negligible discharge of the probe to the solution under investigation for the direct or localized measurement of ROS [10,11]. DNA, 'the molecule of life' has been used extensively for biomaterials development in the last few decades [12]. Among different types of DNA based biomaterials the DNA–lipid (surfactant) complex is most popular [13]. On the other hand, Fiber-Optic Sensors (FOS) are popular since 1987 [14] as FOS based system can be handled by any non-expert with little or no knowledge of instrument handling. In some recent reviews the development of Fiber-Optic Biosensors (FOBS) and Chemical Sensors (FOCS) has also been summarized [15–18]. However, reports on the direct *in-vivo* measurement of ROS or oxidative stress in biological systems are limited in the contemporary literature. There are few reports on potential FOS tools for the detection of hydrogen peroxide [19], with limited portability, cost-effectiveness and versatility. On the other hand there are several reports on the offline measurement of ROS [7,20,21]. However, cost effectiveness and versatility in the measurement capability, which are essential for the conclusive diagnosis of oxidative stress in a physiological condition have been profoundly compromised in the reports. In the given context, development of a highly efficient, portable and inexpensive DNA-based FOS for direct measurement of ROS/oxidative stress in physiologically relevant environments is the motivation of the present work.

In this work, salmon sperm DNA, a waste product of fish-processing industry, is used to produce sensor biomaterial. The highly water soluble DNA forms complex polymers upon interaction with cationic surfactants. The complex is insoluble in water but completely soluble in alcohol [22], which is not only privileged in terms of casting DNA thin-films over any surface but also supreme for sensing applications. We have utilized the exceptional affinity of DNA towards different dyes in order to encapsulate DCFH into the DNA-complex matrix [23]. The DCFH is impregnated into the DNA matrix during the complexation reaction with a cationic surfactant, CTAB (cetyltrimethyl ammonium bromide) in aqueous solution. The DCFH entrapped biomaterial (DNA-DCFH-CTAB complex) eventually dried and re-solubilized in alcohol. We have sensitized a chemically etched fiber tip by dipping the tip into the biomaterial in alcohol solution and dried in air for a minute (dip-coating) for direct measurement of ROS/oxidative stress in physiologically relevant environments. The regenerative use of the fiber tip can be achieved by wiping the fiber tip using ethanol followed by further dip-coating of the tip. Here we have followed the increase in fluorescence intensity and quenching of fluorescence intensity of the sensitized fiber tip upon interaction with well-known ROS generator ( $Mn_3O_4$  nanoparticles: NPs [24]) and ROS quencher (sodium azide:  $NaN_3$  [25]), respectively. The effects of blood phantom (aqueous hemoglobin solution) and real blood (mice model) on the sensitized fiber tip have also been studied.

The fluorescence of sensitized fiber tip gets increased depending upon the concentration of ROS present in the blood phantom/blood samples. Picosecond time-resolved studies on the sensitized fiber tip in presence of ROS with hemoglobin (Hb)/blood samples have confirmed the reabsorption of fluorophores' energy by Hb/blood. In order to assess the effectiveness of the sensor fiber tip, ROS was monitored directly in anaesthetized mice.

## 2. Materials and methods

### 2.1. Materials

In this study analytical grade chemicals were used as received without further purification for synthesis and sample preparation. DNA, CTAB (cetyltrimethyl ammonium bromide; lipid), silicon oil, trisodium citrate ( $Na_3C_6H_5O_7$ ), sodium azide ( $NaN_3$ ), hemoglobin human, copper sulfate pentahydrate ( $CuSO_4 \cdot 5H_2O$ ) and hydro fluoric acid (HF) were obtained from Sigma-Aldrich (USA). Ethanol, hydrogen peroxide ( $H_2O_2$ ; 30%) and sulfuric acid ( $H_2SO_4$ ) were obtained from Merck (NJ, USA). DCFH-DA (2,7-dichlorodihydrofluorescein diacetate) was obtained from Calbiochem. Milli-Q (from Millipore) water was used throughout the experiments. Bifurcated optical fiber, SMA connector and other optical components were purchased from Ocean Optics, USA. For the sensor development, we used multimode silica core fiber (FT1000UMT) from Thorlabs, USA. 'F-3000 Fiber Optic Mount' (Jobin Yvon, HORIBA) was used as an external attachment with the fluorimeter for experiment.

### 2.2. Methods

#### 2.2.1. Synthesis of citrate functionalized $Mn_3O_4$ nanoparticles

Synthesis of bulk  $Mn_3O_4$  NPs was carried out following a reported ultrasonic-assisted approach for preparation of colloidal  $Mn_3O_4$  NPs at room temperature and pressure without any additional surfactants or templates [26]. We followed earlier reports [24,27] for surface functionalization of the bulk NPs with citrate ligand. In brief, as prepared bulk  $Mn_3O_4$  NPs were added to 0.5 M aqueous ligand (citrate) solution of pH 7.0 (~20 mg  $Mn_3O_4$  NPs/mL ligand solution) and were extensively mixed for 12 h in a cyclomixer. A syringe filter of 0.22  $\mu m$  pore diameter was used to eliminate the non-functionalized bigger-sized NPs. The resulting filtrated solution was used for all successive experiments without further dilution. The final concentration of the as prepared functionalized NPs was estimated to be 250  $\mu M$  [28]. Our earlier studies showed the average particle size distribution of the prepared citrate functionalized NPs to be around 3.6 nm  $\pm$  0.15 nm [24,27,28].

#### 2.2.2. Preparation of DNA-based biomaterial

The DNA-based biomaterial (DNA-DCFH-CTAB) was prepared with minute modification of the procedure reported earlier [10]. For preparation of biomaterial, firstly DCFH was prepared from the DCFH-DA by mixing 0.5 mL of 1.0 mM DCFH-DA in methanol with 2.0 mL of 10 mM NaOH at room temperature for 30 min, then the mixture was neutralized with 10 mL of 25 mM  $NaH_2PO_4$  [29]. After that, the DNA stock was prepared by dissolving the fiber-like NaDNA in 50 mM phosphate buffer (6.5 g/mL), and incubated overnight at room temperature in stirring condition. For the preparation of the DNA-DCFH-CTAB complex, the as-prepared 2 mL DCFH (Fig. 1) was added to a 10 mL volumetric flask containing 3 mL of stock DNA solution and 5 mL Milli-Q water. The DNA, DCFH mixture was kept in dark for 60 min under stirring condition at room temperature for complete complexation reaction. Under continuous stirring condition 500  $\mu L$  of 40 mM CTAB solution (in water) was added into the DNA-DCFH mixture. The DNA-DCFH-CTAB complex

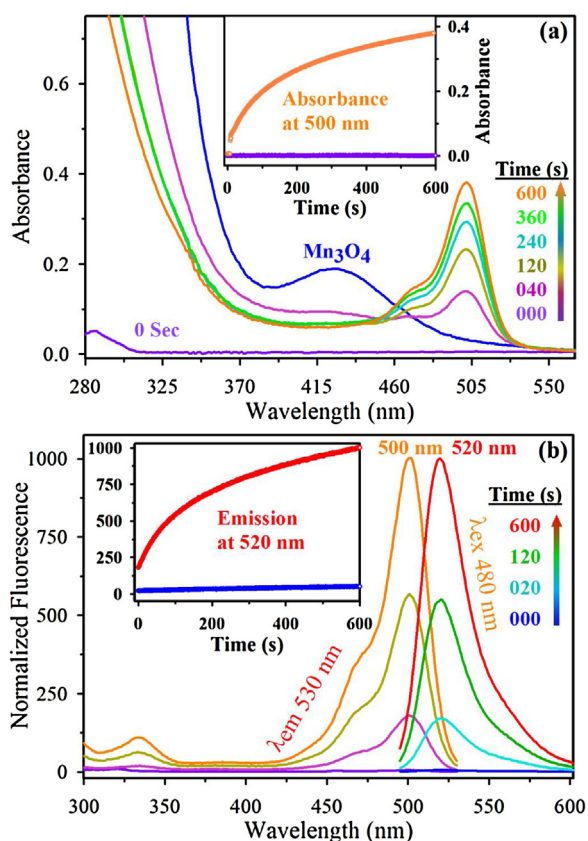


**Fig. 1.** (a) UV-vis absorption spectra of DCFH in presence of Mn<sub>3</sub>O<sub>4</sub> NPs with time and Mn<sub>3</sub>O<sub>4</sub> NPs (Blue) in aqueous medium. Inset shows the reaction kinetics of DCFH in presence and absence of Mn<sub>3</sub>O<sub>4</sub> NPs. (b) Steady-state fluorescence emissions ( $\lambda_{\text{ex}} = 480 \text{ nm}$ ) and excitation ( $\lambda_{\text{em}} = 530 \text{ nm}$ ) spectra of DCFH in absence and presence of ROS generator NPs (Mn<sub>3</sub>O<sub>4</sub>) with time. It has to be noted that the emission peak of DCFH appears at 520 nm. The excitation spectra are collected at detection wavelength of 530 nm to measure complete pattern. Inset shows the reaction kinetics of DCFH in absence and presence of ROS generator NPs. (For interpretation of the references to colour in this figure legend, the reader is referred to the web version of this article.)

started to form spontaneously and accumulated around the stirring bid. The precipitate was collected by filtration, washed with Milli-Q water and then lyophilized overnight. The resultant biomaterial was dissolved in ethanol through vortexing for 30–60 min. The water insoluble DNA-DCFH-CTAB complex was formed due to the binding of CTAB cationic polar head to the negative phosphate sugar chain of the DNA strands. The prepared biomaterial was stored at  $-20^\circ\text{C}$  and used without further modifications. For dip coating an alcohol solution of the biomaterial was prepared for further use. The preparation of DNA-based biomaterial is shown schematically in Fig. 2(a).

### 2.2.3. Fiber tip preparation and sensitization with DNA-biomaterial

The optical fibers of 10 cm length were taken for the sensitization with biomaterial. After removal of jacket (manual etching) from the tip ( $\sim 1 \text{ cm}$ ), the fibers were dipped (the tip portion) into HF solution with a layer of silicone oil atop the solution and kept overnight [30,31]. The chemical etching of the fibers led to a sharp needle like fiber tip as shown in Figs. 2(a) and 3. The etched fiber tip was then coated with the biomaterial by dipping into the biomaterial alcohol solution and dried in air for a minute (dip-coating). The overall fiber tip preparation and sensitization with the biomaterial is shown schematically in Fig. 2(a).

### 2.2.4. Experimental setup

For our study we used a commercially available FluoroLog system with a minute modification of the sample chamber. For the fluorescence-based study a 'F-3000 Fiber Optic Mount' was attached externally to the FluoroLog for transmitting the excitation from the fluorometer and to collect the fluorescence from the tip of the sensitized fiber. Through one end of the Fiber Optic Mount the excitation ( $\lambda_{\text{ex}} = 500 \text{ nm}$ ) was introduced into the sensitized fiber to excite the DCF present in the biomaterial. The green fluorescence of the DCF was collected from another end of the Fiber Optic Mount, which was the signal measured by the fluorometer. All studies were carried out after continuous dipping of the functionalized fiber tip in the samples of interest (Fig. 2(b)). The detailed experimental

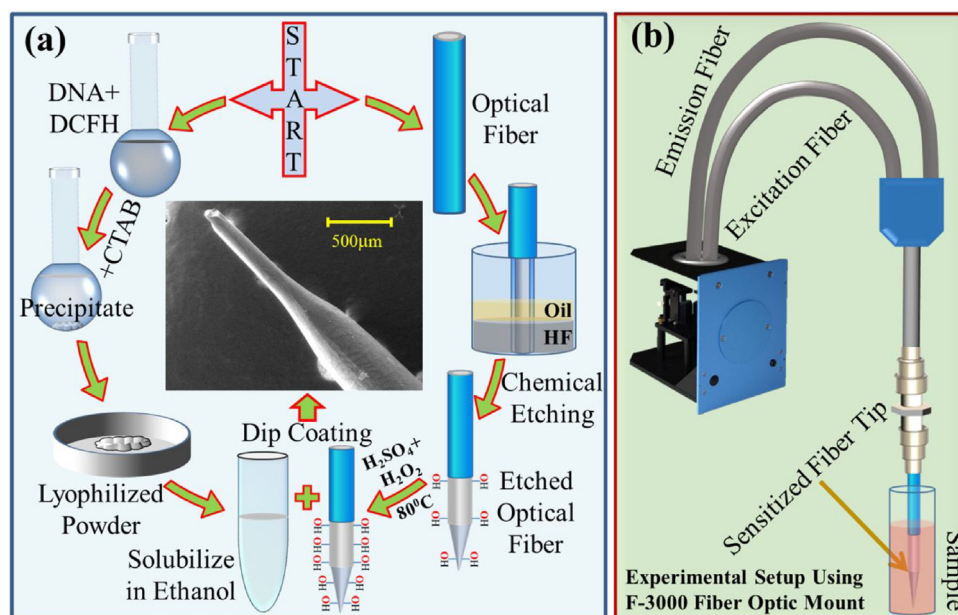


**Fig. 2.** (a) Schematic representation of the DNA-Biomaterial preparation, Optical fiber etching and fiber tip sensitization. Inset shows the SEM image of sensitized fiber tip. (b) Experimental setup using F-3000 Fiber Optic Mount.



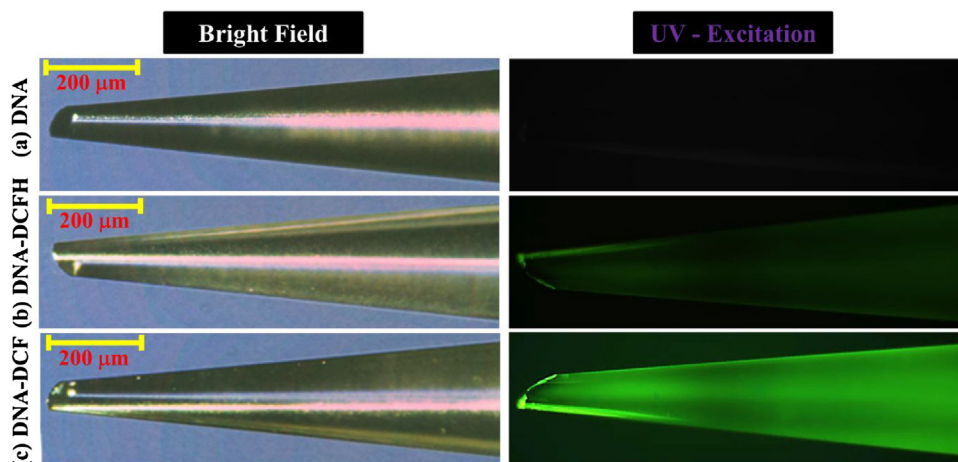


**Fig. 3.** The comparative study of different biomaterial coated fiber tips under bright field (Integration time ( $t$ ) = 50 ms) and UV excitation ( $t$  = 500 ms): (a) DNA coated fiber tip, (b) DNA-Biomaterial coated fiber tip before interaction with NPs, (c) DNA-Biomaterial coated fiber tip after interaction with NPs.

setup using F-3000 Fiber Optic Mount is shown schematically in Fig. 2(b).

### 2.2.5. Optical study

All absorbance and fluorescence measurements were studied using a Shimadzu UV-2600 spectrophotometer and a Horiba FluoroLog fluorimeter, respectively. In order to study the surface morphology of the fiber tip, we used Quanta FEG 250 scanning electron microscope (SEM). The DNA-DCFH-CTAB complex was lyophilized using Heto PowerDry LL1500 Freeze Dryer to get the DNA-based biomaterial as a powder. 'Bright field' and 'Fluorescence' images of the fiber tips were taken using an Olympus BX51 fluorescence microscope. Picosecond-resolved fluorescence transients were carried out using a commercial time correlated single photon counting (TCSPC) setup from Edinburgh Instruments, UK. For 510 nm excitation, we used a picosecond pulsed laser diode with 160 ps instrument response function (IRF). The emission was monitored through a polarizer oriented at  $55^\circ$  with respect to the vertically polarized excitation beam. Curve fitting of the observed fluorescence transients were carried out using a nonlinear least square fitting procedure with multi-exponential ( $n$ ) function [32],

$\sum_{i=1}^n A_i \exp(-t/\tau_i)$  where,  $A_i$ 's are weight percentages of the decay components with time constants of  $\tau_i$ . The average excited state

lifetime is expressed by the equation  $\tau_{avg} = \frac{\sum_{i=1}^n A_i \tau_i}{\sum_{i=1}^n A_i}$

1. The quality of the curve fitting was evaluated by reduced  $\chi^2$  and residual data.

### 2.2.6. Mice treatment protocol

Swiss albino mice of both sexes (4–6 weeks old, weighing  $23 \pm 4$  g) in good physical conditions were used for this study. Animals were kept in standard, clean polypropylene cages (temperature  $22 \pm 3^\circ\text{C}$ ; relative humidity 45–60%; 12 h light/dark cycle). Water and standard laboratory pellet diet for mice (Hindustan Lever, Kolkata, India) were available *ad-libitum*. One week of acclimatization was provided to all of them before the experiment. All animals received human care according to the criteria outlined by the Committee for the Purpose of Control and Supervision of Experiments on Animals (CPCSEA), New Delhi, India, and the study was approved by the Institutional Animal Ethics Committee (approval number IAEC/RES/DEY'S – 12/S/2016 Under Animal Welfare Board, Ministry of Environment Forest and Climate Change, Govt. of India).

In total eight animals were randomized into two groups ( $n=4$  in each group). Group-1 served as sham control and was treated with olive oil (0.5 mL/kg body weight (BW)) in alternative days for a period of 4 weeks. For induction of oxidative stress, Group-2 received carbon tetrachloride solution (25%  $\text{CCl}_4$  in olive oil) 1 mL/kg BW in every alternative days for a period of 4 weeks. All inductions were carried out through intraperitoneal injection. At the end of the experiment, the animals were kept in fasting condition overnight and sacrificed by cervical dislocation. Blood samples were collected in sterile tubes (nonheparinized) from retro orbital plexus just before sacrifice and allowed to clot for 45 min. Serum was separated by centrifugation at 5000 rpm for 15 min. AST and total bilirubin were measured using commercially available test kits (Autospan Liquid Gold, Span Diagnostics Ltd., Gujarat, India) following the protocols described by the corresponding manufacturers. MDA content was determined following the protocol described elsewhere [33]. SOD and Catalase activity were measured using commercially available test kit (Sigma, USA) following the included protocol.

### 2.2.7. Direct in-vivo oxidative stress measurement procedure in mice model

For the purpose of this study, first the sensitized fiber tip was fixed in an anticoagulated capillary tube. Then for the comparative study, data were collected from both normal (control) as well as  $\text{CCl}_4$  induced mice. General anaesthesia was used before performing direct ROS measurement in mice model. For the measurement, the mouse was restrained in such a manner that it cannot move, but was breathing well. Then the eyelid was gently pulled back from the globe and the capillary tube with sensitized fiber tip was gently inserted between the lid and the globe, pushing backward with even pressure, puncturing the conjunctiva, and gaining access to the retro orbital plexus. The blood was then allowed to drip on the surface of sensor tip, inside the capillary tube, by capillary action.

### 2.2.8. Statistical analysis

All quantitative data are expressed as mean  $\pm$  standard deviation (SD) unless otherwise stated. Unpaired  $t$ -test (parametric) following Welch's correction is executed for comparison of different parameters between the groups using GraphPad Prism (version 5.00 for Windows), GraphPad Software (CA, USA).  $p < 0.01$  is considered to be significant.

### 3. Results and discussion

#### 3.1. ROS generation activity of $Mn_3O_4$ nanoparticles

In this study we used citrate functionalized  $Mn_3O_4$  nanoparticles as a ROS generating agent [26]. The UV-vis spectra of the as prepared NPs (200  $\mu$ L in 2 mL water: 25  $\mu$ M) is shown in Fig. 1(a) (blue color). The absorbance maxima at around 290 nm (data not shown) and 429 nm correspond to the high-energy ligand-to-metal charge transfer transition (LMCT) involving citrate-Mn<sup>4+</sup> interaction and Jahn-Teller (J-T) distorted d-d transitions centered over Mn<sup>3+</sup> ions respectively [24]. In order to observe the ROS generation ability of the NPs in aqueous media a fluorescent probe DCFH was employed. Oxidation of DCFH by ROS, converts the molecules to DCF, which is highly fluorescent. The prepared DCFH solution was characterized by the absorbance as well as the fluorescence spectra. Fig. 1(a) shows that the absorbance of DCFH at around 500 nm is increasing with time from zero to finite values in presence of NPs. For more convenience the time dependant change in absorbance of DCFH at 500 nm in presence and absence of NPs are shown in the inset of Fig. 1(a). In addition the excitation spectra of DCFH monitored at 530 nm with time is shown in Fig. 1(b). Fig. 1(b) also reveals the strong emission of DCFH at around 520 nm, upon excitation at 480 nm, in presence of NPs. The above results indicate that the NPs are efficient generator of ROS, which oxidise the non-fluorescent DCFH to highly fluorescent DCF. In order to investigate the ROS generation efficiency of the NPs, the time dependant fluorescence at 520 nm of the DCFH in presence and absence of NPs is observed (inset of Fig. 1(b)). The observed result indicates that the NPs can efficiently generate ROS for more than 15 min.

#### 3.2. Characterization of the DNA-based biomaterial coated fiber tips

After preparation of the biomaterial and the fiber tip, the DNA-based biomaterial was coated on the etched fiber tip by dip-coating. The SEM image of the biomaterial coated fiber tip (sensor tip) confirmed the sharp needle like shape of the sensitized fiber tip (Fig. 2(a)). The comparative microscopic images of different biomaterial coated fiber tips under bright field (Integration time (t) = 50 ms) and UV excitation (t = 500 ms) are presented in Fig. 3. We considered three variants of the biomaterial for our study namely (a) DNA, (b) DNA-DCFH and (c) DNA-DCF (CTAB was common for all). As shown in Fig. 3, all the observations under bright field were almost the same. However, under UV excitation the fiber tip in the panel (a) was invisible and those in panels (b) & (c) were visible. Though the concentration of biomaterial present in both the fiber tips ((b) & (c)) were same but tip shown in panel (c) fluoresces exceptionally high due to the interaction with NPs. Because in presence of NPs (ROS generator) very low-fluorescent DNA-DCFH was converted to highly fluorescent DNA-DCF.

The indigenously developed experimental setup was used to collect the spectroscopic signal from the biomaterial coated fiber tip, as shown in Fig. 2(b). The emission and excitation spectra of the biomaterial coated fiber tip were recorded under the experimental setup (Fig. 2(b)) are represented in Fig. 4(a). A low green (530 nm) emission was observed from the sensitized fiber tip upon excitation at 500 nm wavelength. However, no emission was observed from the fiber tip before sensitization. The excitation spectra corresponding to  $\lambda_{em} \sim 540$  nm reveals the excitation wavelength maxima to be at around 510 nm. The emission maximum of the DCF was shifted from 520 nm (in methanol) to 530 nm (in DNA-matrix) due to the solvent effect. Significant increase in emission/excitation intensity of the biomaterial coated fiber tip after interaction with  $Mn_3O_4$  NPs was due to the ROS generation in the solution by NPs. DCFH present in the biomaterial on the sensitized fiber tip, on oxi-

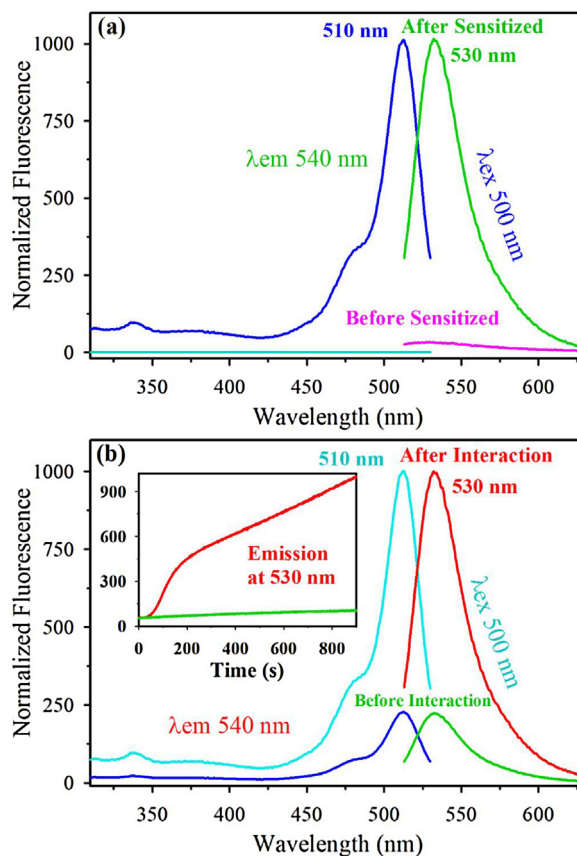


**Fig. 4.** Steady state fluorescence emissions ( $\lambda_{ex}=500$  nm) and excitation ( $\lambda_{em}=540$  nm) of: (a) the fiber tip before and after sensitization with DNA-based biomaterial. (b) the sensitized fiber tip before and after interaction with  $Mn_3O_4$  NPs. Inset shows the fluorescence kinetic of the sensitized fiber tip in absence and presence of  $Mn_3O_4$  NPs.

dation by ROS forms DCF showing an emission maximum at 530 nm is represented in Fig. 4(b). Inset of Fig. 4(b) reveals that the fluorescence intensity of the sensitized fiber tip is increasing with time due to the continuous oxidation of DCFH by the NPs in the test solution and is found to increase up to about 8 fold within 15 min. The persistent increase in DCF fluorescence represents the continuous ROS measurement ability of the sensor tip.

#### 3.3. ROS measurements in aqueous media

Different measurement times are reported in the literature for using DCFH assay for ROS measurements, spanning from minutes to one hour [34,35]. As shown in Fig. 5, we investigated the fluorescence kinetics of the sensor tip over 15 min of exposure to ROS generator (NPs) with different concentrations. As demonstrated in Fig. 5(a), we observed an increase in ROS generation with increasing concentrations of NPs in the solution without any saturation in the fluorescence intensity. The observation reveals that the probe fiber tip would be able to monitor the status of ROS of a given medium for at least 15 min continuously. A control study on the probe fiber tip dipped into water is also shown in Fig. 5(a), revealing negligibly small auto-oxidation of DCFH in the biomaterial. In another controlled experiment we confirmed that the fluorescence kinetics of the sensor tip after dipping into water for 1 h shows comparable kinetic profile with respect to undipped tip. The observation concludes a negligible leaching of the biomaterial including entrapped DCFH to the solution under investigation. In order to confirm the increased oxidative stress in the solution containing NPs, we used sodium azide ( $NaN_3$ ), which is a

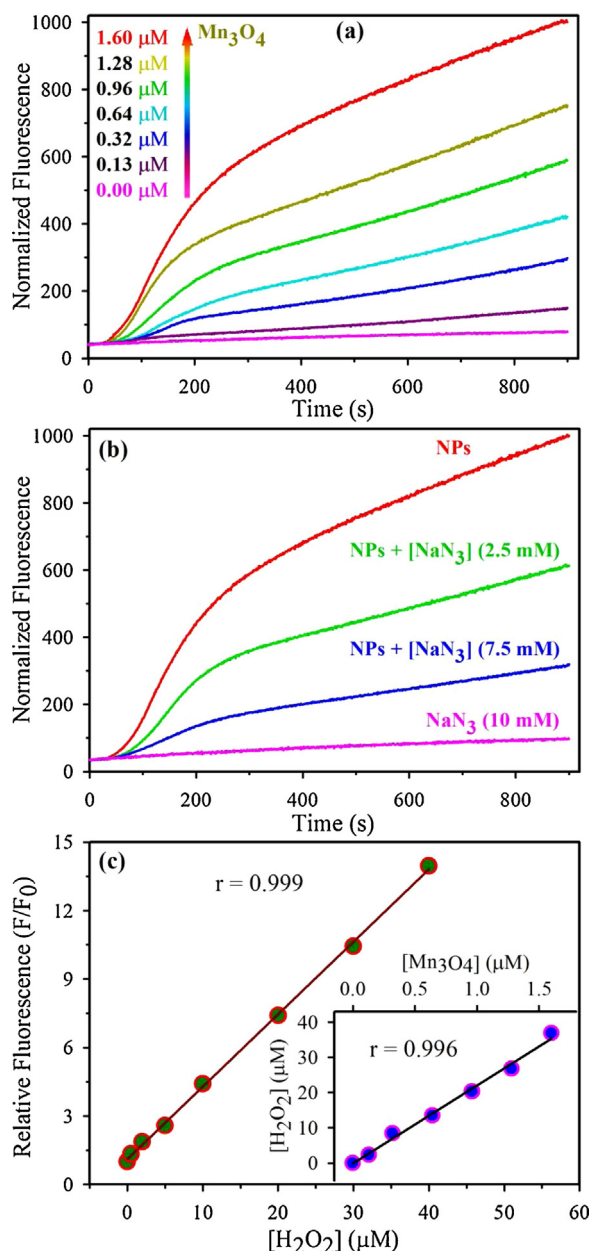


**Fig. 5.** The fluorescence kinetics (emission at 530 nm) of the sensitized fiber tip: (a) with increasing concentrations of NPs (ROS generator), (b) with increasing concentrations of  $\text{NaN}_3$  (ROS quencher) keeping fixed NPs concentration (1.60  $\mu\text{M}$ ). (c) Calibration curve of relative fluorescent intensity obtained from the reaction between DCFH and  $\text{H}_2\text{O}_2$  in presence of constant  $\text{Cu}^{2+}$  ions (150  $\mu\text{M}$ ) with incubation time 15 min. The linear dependency is remarkable. Inset shows the relation between concentration of NPs and equivalent  $\text{H}_2\text{O}_2$  concentration estimated from relative DCF fluorescence. Note the linear relationship in this case also.

well-known ROS quencher in aqueous solution [25]. As shown in Fig. 5(b), the extent of fluorescence enhancement in the sensor fiber tip decreased with the increase in  $\text{NaN}_3$  concentration in the test solution at a fixed NPs concentration (ROS generator). Therefore, the nature of ROS was found to be singlet oxygen, as the oxidation of DCFH decreased significantly in presence of  $\text{NaN}_3$ , a well-known singlet oxygen quencher [25,33]. In order to get a quantitative estimation of ROS in various environments including mice blood, we calibrated the fluorescence enhancement of DCF in presence of different measured amounts of  $\text{H}_2\text{O}_2$ , a well-known ROS source in presence of  $\text{Cu}^{2+}$  ions [25]. Thus the concentration of ROS measured in our developed sensor tip is essentially equivalent to the

concentration of  $\text{H}_2\text{O}_2$  [36]. Fig. 5(c) shows the calibration relationship between the relative fluorescence intensity ( $F/F_0$ :  $F$  is the fluorescence intensity of DCF in presence of ROS generator and  $F_0$  is the fluorescence intensity of DCF in absence of ROS generator) and  $\text{H}_2\text{O}_2$  concentration in presence of constant  $\text{Cu}^{2+}$  ions (150  $\mu\text{M}$ ). The calibration equation obtained from the linear regression curve is  $F/F_0 = 0.317 \times [\text{H}_2\text{O}_2] + 1.11$ , with the Pearson's correlation coefficient  $r = 0.999$ . We also calibrated the concentration of the NPs used in our present study as ROS generator in terms of equivalent  $\text{H}_2\text{O}_2$  concentration using the relative fluorescence of DCF in the corresponding solution as shown in the inset of Fig. 5(c). As shown in the figure, the estimated ROS concentration values in the aqueous medium generated by 0.13, 0.32, 0.64, 0.96, 1.28, and 1.60  $\mu\text{M}$  NPs are found to be 2.30, 8.48, 13.54, 20.27, 26.84 and 36.85  $\mu\text{M}$ , respectively.

### 3.4. ROS/Oxidative stress measurement in blood phantom and mice blood

Direct measurement of oxidative stress in physiological milieu is very difficult due to following two important factors. Firstly, the concerned ROS are having very short lifetime [37] revealing erroneous results upon detachment of test sample (e.g. blood) from the main body. This fact requires an *In-vivo* placement of the sensor probe to the main body. Secondly, the reaction of the sensor probe with the test sample reveals toxicity in the main body during the measurements. *In-vivo* measurements require a non-toxic sensor probe for the measurement of oxidative stress in physiological milieu. Thus, oxidative stress assessment is usually performed by indirect methods measuring ROS-induced oxidative damages on proteins, membrane lipids, and DNA, the most vulnerable biological targets for oxidative stress [38]. Although thousands of articles have been attributed for evaluation of oxidative damage by measuring the increase of protein oxidation, direct measurement of ROS in the biological system is still missing. Here we choose blood as a system for direct monitoring of ROS levels. It is well known that red blood cells (RBC) may exert both antioxidant and pro-oxidant activity because of the high-iron concentration [38]. Keeping this fact in mind we select hemoglobin (Hb) solution as a blood phantom for examining its pro and antioxidant activity. Fig. 6(a) reveals that the fluorescence intensity of the developed sensor tip significantly increases with time in presence of Hb compared to that in control sample (water). The observation is consistent with the pro-oxidant activity of Hb in the proximity of the sensor probe. It is also reported that Hb shows antioxidant properties in environment with high oxidative stress [39]. Fig. 6(a) presents how the ROS generation ability of NPs is reduced due to the presence of Hb in the solution. The Fig. also shows that even in the presence of fixed concentration of ROS generator NPs (1.28  $\mu\text{M}$ ) the oxidation of DCFH was dramatically decreased with increasing concentration of Hb resulting in a decrease in the fluorescence intensity of the sensor tip. The above results reveal that the developed sensor tip is able to efficiently measure the presence of ROS, the major cause of oxidative stress in blood phantom.

In order to measure the oxidative stress in real blood, blood samples were collected from retro-orbital sinus plexus of Swiss albino mice. Freshly obtained blood samples were immediately diluted into two different ways and stored on ice prior to analysis. For sample 1, 5  $\mu\text{L}$  of fresh blood was diluted in 4 mL of phosphate buffered saline water. For sample 2, 5  $\mu\text{L}$  of the same blood was diluted in 4 mL of phosphate buffered saline water in presence of different concentrations of oxidant (NPs). The ROS measurement study was carried out with our indigenously developed setup (Fig. 2) using the prepared samples. As shown in Fig. 6(b), the fluorescence intensity (at 530 nm) of the sensor fiber increases significantly in sample 1 compared to that in buffer solution. The study demonstrates the



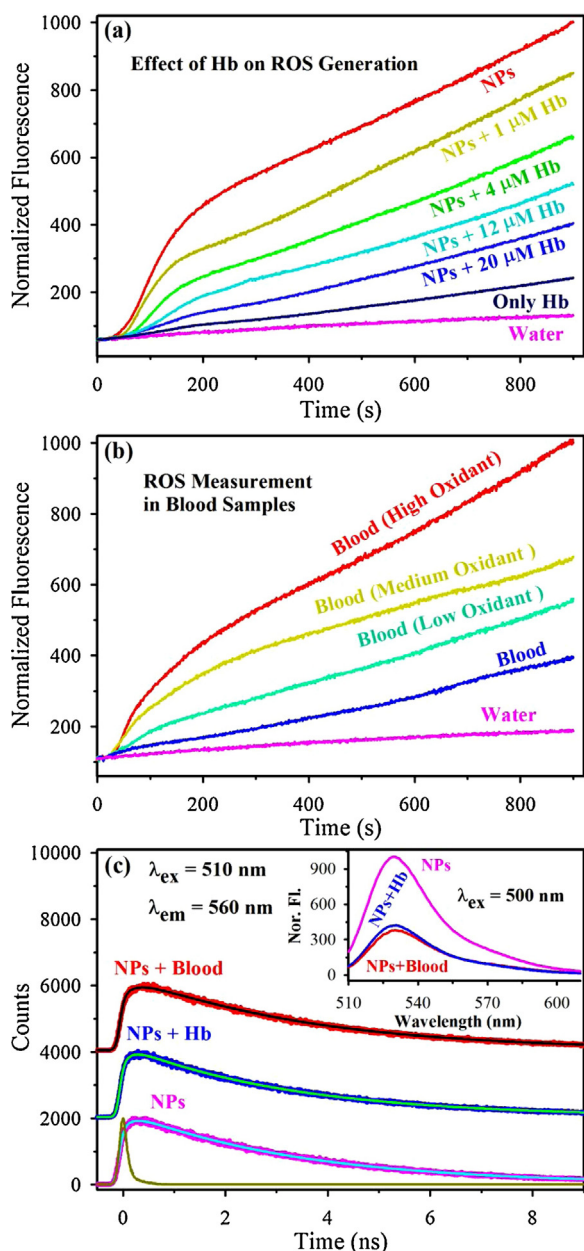


**Fig. 6.** (a) The effect of Hb concentration on fluorescence kinetics of the sensor tip with fixed oxidant (NPs) concentration (1.28  $\mu\text{M}$ ). (b) Oxidative stress measurement in mice blood with different concentrations of oxidant (NPs). (c) Picosecond time-resolved fluorescence transients of the sensor tip in presence of NPs, NPs + Hb, and NPs + Blood upon excitation at 510 nm. Inset shows the corresponding steady-state fluorescence spectra.

pro-oxidant activity of the whole blood. Fig. 6(b) also shows that the fluorescence intensity of the DCF in presence of sample 2 increases with increasing oxidant (NPs) concentration for a fixed concentration of blood in the medium. The observation is consistent with the fact, that the developed sensor would be able to measure oxidative stress and its different extents in real blood sample.

The inset of Fig. 6(c) presents the steady-state fluorescence of the sensor fiber in presence of NPs (ROS generator), Hb + NPs and whole blood + NPs in aqueous solution. A significant quenching of the fluorescence intensity in presence of Hb and whole blood is evident. In order to unravel the photophysical basis of the fluorescence quenching, we performed picosecond resolved fluorescence transient measurement monitored at 560 nm (excitation 510 nm) as shown in Fig. 6(c). The fluorescence transients of sensor tip in

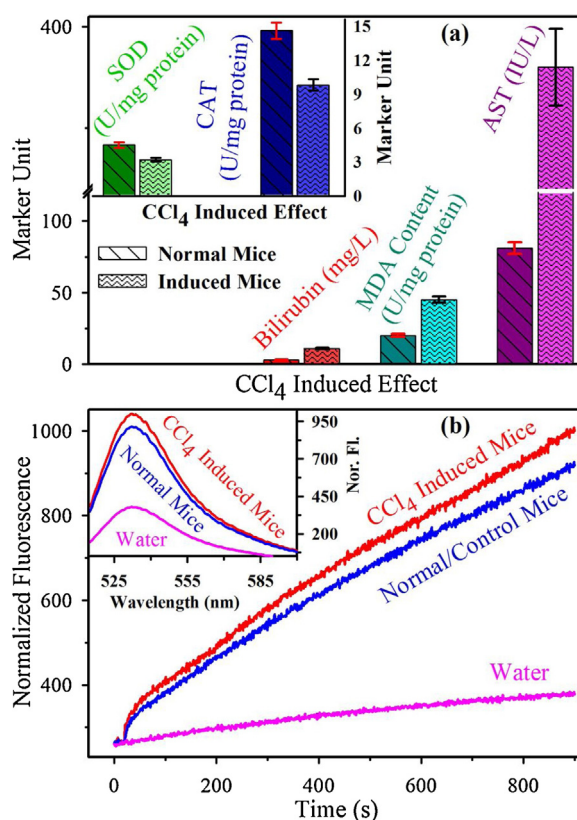


**Fig. 7.** (a) Comparison of conventional biomarker levels (serum and liver function parameters), which are used to evaluate the oxidative damage, between the normal (control) and  $\text{CCl}_4$  induced mice. (b) Direct *in-vivo* measurement of oxidative stress in mice model by the developed fiber optics sensor. Inset shows the corresponding steady state fluorescence spectra of the direct *in-vivo* measurement at the end (after 15 min).

presence of NPs exposed single-exponential time constants with lifetime ( $\tau$ ) of 3.4 ns, which remained unchanged in the presence of Hb and whole blood. The results rule out any kind of excited state processes including electron transfer and/or complexation of the biomaterial on the fiber tip and Hb/blood in the aqueous medium, other than mere re-absorption of the fiber tip emission by the Hb/whole blood [40].

### 3.5. Direct *in-vivo* measurement of oxidative stress in mice model

In order to validate the developed sensor in preclinical model, we induced mice with  $\text{CCl}_4$  to generate oxidative stress [33]. To confirm the induction of oxidative stress in the  $\text{CCl}_4$  induced mice, we evaluated some serum parameters (SOD, Catalase, AST, Total Bilirubin and Lipid Peroxidation) which are conventionally considered as the potential biomarkers [33]. SOD and Catalase are the two mutually supportive kingmakers of *in-vivo* antioxidant defence system. SOD converts superoxide anions to  $\text{H}_2\text{O}_2$ , which is further converted to  $\text{H}_2\text{O}$  with the help of GPx and CAT. SOD also inhibits hydroxyl radical production. In our study, as shown inset of Fig. 7(a),  $\text{CCl}_4$  caused substantial downregulation of the SOD ( $\sim 28.9\%$ ) and CAT ( $\sim 32.9\%$ ) activities, indicating the introduction of high oxidative stress. We further studied the effect of  $\text{CCl}_4$  on liver function parameters as the liver serves as the primary target organ of this genotoxic agent. Fig. 7(a) presents both AST ( $\sim 369.1\%$ ) and total bilirubin level ( $\sim 266.7\%$ ) were much higher than the respective control groups; further signifying that free radicals induced severe liver damage. Rapid lipid peroxidation of the membrane structural lipids was proposed as the basis of  $\text{CCl}_4$  liver

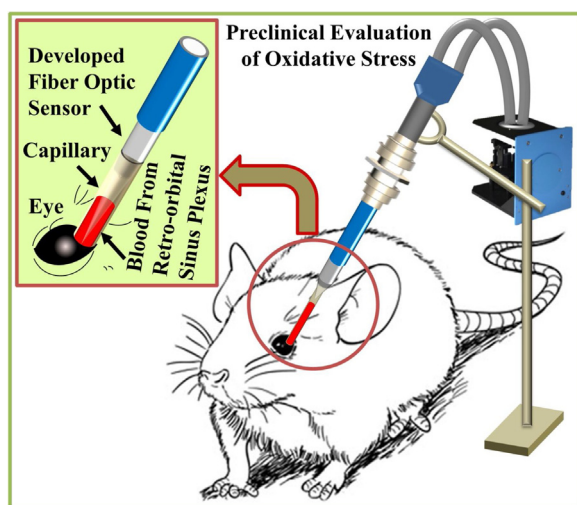
**Table 1**  
Comparison of various oxidative stress markers between Normal and CCl<sub>4</sub> intoxicated mice.

Marker	Normal mice	CCl <sub>4</sub> induced mice	Change in%	p value
SOD (U/mg protein)	4.5 ± 0.3	3.2 ± 0.4	28.9	0.0025
CAT (U/mg protein)	14.6 ± 1.2	9.8 ± 1.1	32.9	0.0011
AST (IU/L)	81 ± 5.2	380 ± 40.1	369.1	0.0006
BILIRUBIN (mg/dL)	0.3 ± 0.04	1.1 ± 0.05	266.7	0.0001
MDA Content (mmoles/mg protein)	20 ± 3.1	45 ± 4.2	125.0	0.0014
Measured ROS (μM) using the proposed method	4.16 ± 0.12	5.00 ± 0.20	20.2	0.0009

Data are expressed as mean ± standard deviation (n = 4).

p value computed using unpaired t-test (parametric) with Welch's correction.

\*p < 0.01 compared to Normal mice.

**Scheme 1.** Schematic representation of the direct *in-vivo* measurement of oxidative stress in mice model by the developed fiber optics sensor.

toxicity. So, we monitored the levels of MDA, an index of oxidative damage and one of the decomposition products of peroxidised polyunsaturated fatty acids, to evaluate the effect of CCl<sub>4</sub> induction. As shown in Fig. 7(a), significant increase of MDA (~125.0%) in the CCl<sub>4</sub>-treated group strongly confirmed that the substantial oxidative damage had been induced. All the results are tabulated in Table 1. The direct *in-vivo* measurements of oxidative stress in both normal (control) as well as CCl<sub>4</sub> –treated mice were carried out by our developed sensor for the comparisons (data were collected following the describe method (Section 2.2.6) using the developed setup (Fig. 2(b))). The obtained results were then validated with the conventional biomarker levels which are used to evaluate the oxidative damage as mentioned above. As shown in Fig. 7(b), the collected fluorescence intensity (at 530 nm, up to 15 min) of the sensor from the CCl<sub>4</sub> induced mice is significantly different compared to the control one (normal mice) at every time. The difference is evident in the steady state fluorescence spectra also, as shown inset of Fig. 7(b). The concentration of ROS in the CCl<sub>4</sub> induced and normal mice are estimated to be 5.00 ± 0.20 μM and 4.16 ± 0.12 μM respectively (p < 0.01). The direct *in-vivo* measurement of oxidative stress in mice model is shown schematically in the Scheme 1. The above facts indicate the sensor result is well consistent with the conventional biomarker levels for evaluation of oxidative stress. The observed results also confirm the direct *in-vivo* oxidative stress measurement ability of the developed sensor in the living animal models. Although a thorough study for direct *in-vivo* oxidative stress measurement is under investigation, the proof of concept experiment clearly showed a promise for the direct *in-vivo* measurement of oxidative stress.

## 4. Conclusions

In summary, we have developed a DNA-based portable fiber optic sensor for the direct *in-vivo* measurement of oxidative stress in physiological milieu. Impregnated DCFH assay in a water insoluble DNA-lipid complex at the sensitized tip of a multimodal optical fiber is shown to play a crucial role in the sensing mechanism. Significant increase in fluorescence intensity of the indigenously developed biomaterial functionalized fiber tip is shown to be a key factor for the aforementioned sensing. Moreover, the sensor is shown to monitor ROS/oxidative stress efficiently and continuously in the aqueous medium as well as in the biological samples, without forming any complexations or reaction with the biological samples. To our understanding, the scope for further development of the concept is extensive, which offers great potential for the development of economical, portable devices for the direct *in-vivo* measurement of oxidative stress efficiently. In the future, our study is expected to find relevance in the quick measurement of oxidative stress in human subjects in a minimally invasive way.

## Disclosures

The authors have disclosed no conflicts of interest.

## Acknowledgements

P.K.S. is thankful to UGC (India) for providing the fellowship under the UGC-RGNF scheme. We are also thankful to ICMR for financial support (5/3/8/247/2014ITR) and DBT (India) for Financial Grant BT/PR11534/NNT/28/766/2014. We thank NTH-School “Contacts in Nanosystems: Interactions, Control and Quantum Dynamics” and DFG-RTG 1952/1, Metrology for Complex Nanosystems.

## References

- [1] B. Kalyanaraman, V. Darley-Usmar, K.J.A. Davies, P.A. Dennery, H.J. Forman, M.B. Grisham, et al., Measuring reactive oxygen and nitrogen species with fluorescent probes: challenges and limitations, *Free Radic. Biol. Med.* 52 (2012) 1–6.
- [2] V.J. Hammond, J.W. Aylott, G.M. Greenway, P. Watts, A. Webster, C. Wiles, An optical sensor for reactive oxygen species: encapsulation of functionalised silica nanoparticles into silicate nanopores to reduce fluorophore leaching, *Analyst* 133 (2007) 71–75.
- [3] J.T. Hancock, R. Desikan, S.J. Neill, Role of reactive oxygen species in cell signalling pathways, *Biochem. Soc. Trans.* 29 (2001) 345.
- [4] Helena M. Cochemé, C. Quin, Stephen J. McQuaker, F. Cabreiro, A. Logan, Tracy A. Prime, et al., Measurement of H<sub>2</sub>O<sub>2</sub> within living drosophila during aging using a ratiometric mass spectrometry probe targeted to the mitochondrial matrix, *Cell Metab.* 13 (2011) 340–350.
- [5] S. Martins, J.P.S. Farinha, C. Baleizao, M.N. Berberan-Santos, Controlled release of singlet oxygen using diphenylanthracene functionalized polymer nanoparticles, *Chem. Commun.* 50 (2014) 3317–3320.
- [6] M. Karlsson, T. Kurz, Ulf T. Brunk, Sven E. Nilsson, Christina I. Frennesson, What does the commonly used DCF test for oxidative stress really show? *Biochem. J.* 428 (2010) 183.



- [7] J.M. Burns, W.J. Cooper, J.L. Ferry, D.W. King, B.P. DiMento, K. McNeill, et al., Methods for reactive oxygen species (ROS) detection in aqueous environments, *Aquat. Sci.* 74 (2012) 683–734.
- [8] J. Chan, S.C. Dodani, C.J. Chang, Reaction-based small-molecule fluorescent probes for chemoselective bioimaging, *Nat. Chem.* 4 (2012) 973–984.
- [9] A.R. Lippert, G.C. Van de Bittner, C.J. Chang, Boronate oxidation as a bioorthogonal reaction approach for studying the chemistry of hydrogen peroxide in living systems, *Acc. Chem. Res.* 44 (2011) 793–804.
- [10] N. Polley, P.K. Sarkar, S. Chakrabarti, P. Lemmens, S.K. Pal, DNA biomaterial based fiber optic sensor: characterization and application for monitoring in situ mercury pollution, *ChemistrySelect* 1 (2016) 2916–2922.
- [11] S. Heng, M.-C. Nguyen, R. Kostecki, T.M. Monro, A.D. Abell, Nanoliter-scale regenerable ion sensor: sensing with a surface functionalized microstructured optical fibre, *RSC Adv.* 3 (2013) 8308–8317.
- [12] A.J. Steckl, DNA – a new material for photonics? *Nat. Photon.* 1 (2007) 3–5.
- [13] K. Tanaka, Y. Okahata, A DNA-lipid complex in organic media and formation of an aligned cast film, *J. Am. Chem. Soc.* 118 (1996) 10679–10683.
- [14] C.A. Villarruel, D.D. Dominguez, A. Dandridge, Evanescent wave fiber optic chemical sensor, *Proc. SPIE* (1987) 225–229.
- [15] O.S. Wolfbeis, Fiber-optic chemical sensors and biosensors, *Anal. Chem.* 80 (2008) 4269–4283.
- [16] X.-D. Wang, O.S. Wolfbeis, Fiber-optic chemical sensors and biosensors (2008–2012), *Anal. Chem.* 85 (2013) 487–508.
- [17] M. Pospíšilová, G. Kuncová, J. Trögl, Fiber-optic chemical sensors and fiber-optic bio-sensors, *Sensors* 15 (2015) 25208.
- [18] X.-d. Wang, O.S. Wolfbeis, Fiber-optic chemical sensors and biosensors (2013–2015), *Anal. Chem.* 88 (2016) 203–227.
- [19] M. Purdey, J. Thompson, T. Monro, A. Abell, E. Schartner, A dual sensor for pH and hydrogen peroxide using polymer-coated optical fibre tips, *Sensors* 15 (2015) 29893.
- [20] I.-W. Kim, J.M. Park, Y.J. Roh, J.H. Kim, M.-G. Choi, T. Hasan, Direct measurement of singlet oxygen by using a photomultiplier tube-based detection system, *J. Photochem. Photobiol. B* 159 (2016) 14–23.
- [21] S. Hosaka, T. Itagaki, Y. Kuramitsu, Selectivity and sensitivity in the measurement of reactive oxygen species (ROS) using chemiluminescent microspheres prepared by the binding of acridinium ester or ABEI to polymer microspheres, *Luminescence* 14 (1999) 349–354.
- [22] V.G. Sergeev, S.V. Mikhailenko, O.A. Pyshkina, I.V. Yaminsky, K. Yoshikawa, How does alcohol dissolve the complex of DNA with a cationic surfactant? *J. Am. Chem. Soc.* 121 (1999) 1780–1785.
- [23] D. Banerjee, S.K. Pal, Dynamics in the DNA recognition by DAPI: exploration of the various binding modes, *J. Phys. Chem. B* 112 (2008) 1016–1021.
- [24] N. Polley, S. Saha, A. Adhikari, S. Banerjee, S. Darbar, S. Das, et al., Safe and symptomatic medicinal use of surface-functionalized Mn<sub>3</sub>O<sub>4</sub> nanoparticles for hyperbilirubinemia treatment in mice, *Nanomedicine* 10 (2015) 2349–2363.
- [25] M. Bancirova, Sodium azide as a specific quencher of singlet oxygen during chemiluminescent detection by luminol and Cypridina luciferin analogues, *Luminescence* 26 (2011) 685–688.
- [26] S. Lei, K. Tang, Z. Fang, H. Zheng, Ultrasonic-assisted synthesis of colloidal Mn<sub>3</sub>O<sub>4</sub> nanoparticles at normal temperature and pressure, *Cryst. Growth Des.* 6 (2006) 1757–1760.
- [27] A. Giri, N. Goswami, M. Pal, M.T. Zar Myint, S. Al-Harathi, A. Singha, et al., Rational surface modification of Mn<sub>3</sub>O<sub>4</sub> nanoparticles to induce multiple photoluminescence and room temperature ferromagnetism, *J. Mater. Chem. C* 1 (2013) 1885–1895.
- [28] A. Giri, N. Goswami, C. Sasmal, N. Polley, D. Majumdar, S. Sarkar, et al., Unprecedented catalytic activity of Mn<sub>3</sub>O<sub>4</sub> nanoparticles: potential lead of a sustainable therapeutic agent for hyperbilirubinemia, *RSC Adv.* 4 (2014) 5075–5079.
- [29] S. Sardar, S. Chaudhuri, P. Kar, S. Sarkar, P. Lemmens, S.K. Pal, Direct observation of key photoinduced dynamics in a potential nano-delivery vehicle of cancer drugs, *Phys. Chem. Chem. Phys.* 17 (2015) 166–177.
- [30] B.A.F. Puygranier, P. Dawson, Chemical etching of optical fibre tips – experiment and model, *Ultramicroscopy* 85 (2000) 235–248.
- [31] W. Pak Kin, U. Ulmanella, H. Chih-Ming, Fabrication process of microsurgical tools for single-cell trapping and intracytoplasmic injection, *J. Microelectromech. Syst.* 13 (2004) 940–946.
- [32] P.K. Sarkar, N. Polley, S. Chakrabarti, P. Lemmens, S.K. Pal, Nanosurface energy transfer based highly selective and ultrasensitive turn on fluorescence mercury sensor, *ACS Sens.* 1 (2016) 789–797.
- [33] A. Adhikari, N. Polley, S. Darbar, D. Bagchi, S.K. Pal, Citrate functionalized Mn<sub>3</sub>O<sub>4</sub> in nanotherapy of hepatic fibrosis by oral administration, *Future Sci. OA* 2 (2016) FSO146.
- [34] A.K. Pal, D. Bello, B. Budhlall, E. Rogers, D.K. Milton, Screening for oxidative stress elicited by engineered nanomaterials: evaluation of acellular DCFH assay, *Dose-Res.* 10 (2012) 308–330.
- [35] J.M. Veranth, E.G. Kaser, M.M. Veranth, M. Koch, G.S. Yost, Cytokine responses of human lung cells (BEAS-2B) treated with micron-sized and nanoparticles of metal oxides compared to soil dusts, *Part. Fibre. Toxicol.* 4 (2007), 2–2.
- [36] J. Zhao, P.K. Hopke, Concentration of reactive oxygen species (ROS) in mainstream and sidestream cigarette smoke, *Aerosol Sci. Technol.* 46 (2012) 191–197.
- [37] K. Krumova, G. Cosa, Overview of Reactive Oxygen Species, 2016.
- [38] S. Mrakic-Sposta, M. Gussoni, M. Montorsi, S. Porcelli, A. Vezzoli, A quantitative method to monitor reactive oxygen species production by electron paramagnetic resonance in physiological and pathological conditions, *Oxid. Med. Cell. Longev.* 2014 (2014) 10.
- [39] M. Minetti, W. Malorni, Redox control of red blood cell biology: the red blood cell as a target and source of prooxidant species, *Antioxid. Redox Signal.* 8 (2006) 1165–1169.
- [40] P.K. Sarkar, S. Pal, N. Polley, R. Aich, A. Adhikari, A. Halder, et al., Development and validation of a noncontact spectroscopic device for hemoglobin estimation at point-of-care, *J. Biomed. Opt.* 22 (2017), 055006–055006.

## Biographies

**Probir Kumar Sarkar** is presently working as a PhD scholar under the supervision of Prof. Samir Kumar Pal at S. N. Bose National Centre for Basic Sciences, Kolkata, India. He received his M.Sc. degree in Physics in 2013 from Indian Institute of Technology Kanpur, India. The main focus of his work is on the spectroscopic studies of molecules and nanomaterials for potential applications in medical diagnosis and environmental pollution monitoring.

**Animesh Halder** is presently pursuing PhD under the supervision of Prof. Samir Kumar Pal. He has completed his M. Tech in Bioelectronics from Tezpur University, India, and his B. Tech in Applied Electronics and Instrumentation Engineering from Haldia Institute of Technology, India. His interest includes the design and realization of instrumentation in biomedical studies and waveguide-based sensors.

**Aniruddha Adhikari** is presently working as a PhD scholar under the supervision of Prof. Samir Kumar Pal at S. N. Bose National Centre for Basic Sciences after completing Masters in Biochemistry from University of Calcutta. His research interests include interactions of nanoparticles with living organisms, therapeutic effects of nanomaterials and ethnobotanic substances, structure function dynamics of enzyme substrate interaction and toxicity in nanodomain.

**Nabarun Polley** is currently he is pursuing his PhD under the supervision of Prof. Samir Kumar Pal at S. N. Bose National Centre for Basic Sciences, Kolkata, India graduated in physics (BSc) in 2009 and received a master's degree in biomedical instrumentation in 2011 from the University of Calcutta, India. The main focus of his work is on developing and designing new biomedical tools using spectroscopic techniques.

**Soumendra Darbar** completed his M.Sc. (Physiology) from University of Calcutta & M.Sc. (Ecology & Environment) from Sikim Monipal University. He completed his Ph.D degree from Jadavpur University in Pharmacology & Toxicology. Currently he is working on Drug Developmental Research focused on hepatology, diabetes, cancer, mol-bio., nanomedicine, natural drug therapy. He has 20 years of research experience, 15 years industrial experience, 9 years of teaching experience in university.

**Peter Lemmens** is presently professor in the Institute for Condensed Matter Physics, Institut für Physik der Kondensierten Materie, Braunschweig, Germany. His work relates to the interplay of photons with electronic correlation effects, spin orbit interaction, and nanoscales. He also investigates nanosystems, energy transfer, transition metal oxides and topological systems.

**Samir Kumar Pal** is presently a professor in the Department of Chemical Biological & Macromolecular Sciences, S. N. Bose National Centre for Basic Sciences, Kolkata, India. His fields of interest include experimental biophysics in molecular recognition, bio-nano interface, biomedical instrumentation, and environmental pollution. He has authored more than 210 research papers in various international peer-reviewed journals, has 20 patents, and has authored 5 book chapters.